Beam normal spin asymmetry in the equivalent photon approximation

M. Gorchtein[1, 2]

[1] *Genoa University, Department of Physics, 16146 Genoa, Italy*
[2] *California Institute of Technology, Pasadena, CA 91125, USA**

The two-photon exchange contribution to the single spin asymmetries with the spin orientation normal to the reaction plane is discussed for elastic electron-proton scattering in Regge regime. For this, the equivalent photon approximation is adopted. In this case, hadronic part of the two-photon exchange amplitude describes real Compton scattering (RCS). The imaginary part of helicity conserving RCS amplitudes are related to total photoabsorption cross section. The contribution of the photon helicity flipping amplitudes is estimated by the two pion exchange in the t-channel. We observe the double logarithmic enhancement in the electron mass but find it's contribution to the asymmetry negligibly small in the forward kinematics. These results are in strong disagreement with the existing calculation.

PACS numbers: 12.40.Nn, 13.40.Gp, 13.60.Fz, 14.20.Dh

I. INTRODUCTION

Recently, the new polarization transfer data for the electromagnetic form factors ratio G_E/G_M [1] raised a lot of interest for the two photon exchange (TPE) physics in elastic electron proton scattering. These new data appeared to be incompatible with the Rosenbluth data [2]. A possible way to reconcile the two data sets was proposed [3], which consists in a more precise account on the TPE amplitude, the real part of which enters the radiative corrections to the cross section (Rosenbluth) and the polarization cross section ratio in a different manner. At present, only the IR divergent part of the two photon exchange contribution, corresponding to one of the exchanged photon beeing soft, is taken into the experimental analysis [4]. Two model calculations exist for the real part of the TPE amplitude [5, 6], and they qualitatively confirm that the exchange of two hard photons may be responsible for this discrepancy. In order to extract the electric form factor in the model independent way, one has thus to study the general case of Compton scattering with two spacelike photons. These two photon contributions are important for the electroweak sector, as well.

In view of this interest, parity-conserving single spin asymmetries in elastic ep-scattering with the spin orientation normal to the reaction plane regain an attention. These observables are directly related to the imaginary part of the TPE amplitude and have been an object of theoretical studies in the 1960's and 70's [7]. By analyticity, the real part of the TPE amplitude is given by a dispersion integral over its imaginary part. Therefore, a good understanding of this class of observables is absolutely necessary. Recently, first measurements of the beam normal spin asymmetry B_n[1] have been performed in different kinematics [8].

Though small (several to tens ppm), this asymmetry can be measured with a precision of fractions of ppm. Before implementing different models for the real part, where an additional uncertainty comes from the dispersion integral over the imaginary part, one should check the level of understanding of the imaginary part of TPE. These checks have been done for the existing data. Inclusion of the elastic (nucleon) intermediate state only [9] led to negative asymmetry of several ppm in the kinematics of SAMPLE experiment but was not enough to describe the data. The description of the beam normal spin asymmetry within a phenomenological model which uses the full set of the single pion electroproduction [10] did not give satisfactory description at any of the available kinematics. Especially intriguing appears the situation with the SAMPLE data with electron lab energy $E_{lab} = 200$ MeV, which is just above the pion production threshold where the theoretical input is well understood. On the other hand, an EFT calculation without dynamical pions [11] was somewhat surprisingly very successful in describing this kinematics for B_n. This success suggests that to the given order of chiral perturbation theory, the role of the dynamical pions for this observable might be not too large.

Though even at low energies the situation with the imaginary part of TPE amplitude is by far not clear, an attention has to be paid to high energies, as well, since the dispersion integral which would give us its real part, should be performed over the full energy range. Due to relative ease of measuring B_n within the framework of parity violating electron scattering, new data from running and upcoming experiments [12] will stimulate further theoretical investigations of this new observable. A calculation of B_n in hard kinematics regime at high energy and momentum transfer was performed recently in the framework of generalized parton distributions (GPD's) and resulted in asymmetries of ~ 1.5 ppm. [13].

Since a ppm effect measurement at high momentum transfers is an extremely complicated task, we concen-

*Electronic address: gorshtey@caltech.edu

[1] In the literature, also the A_n notation for beam normal spin asymmetry or vector analyzing power was adopted.

trate in this work on the forward kinematics. For this kinematics, a calculation exists [14], where an observation is made that the contribution of the situation where the exchanged photons are nearly real and overtake the external electron kinematics is enhanced as $\ln^2(-t/m^2)$, with m the electron mass and $t < 0$ the elastic momentum transfer. The authors of [14] take the forward VCS amplitude and DIS structure functions as an input, and provide an estimation of B_n in this kinematics as large as 25-35 ppm. We demonstrate that such a treatment is not adequate and leads to an overestimation of the effect by an order of magnitude for the JLab energy $E_{lab} = 5.77$ GeV. In order to provide an estimate of the contribution of this kinematics to B_n, we use the most general real Compton scattering amplitude. We observe that the double logarithmic enhancement is not a consequence of taking the forward limit but a pure kinematical effect within the loop integral. We demonstrate that this treatment of the problem leads to much smaller values for this asymmetry than those quoted in [14]. We provide furthermore a clear explanation of this discrepancy. In fact, it is a consequence of the well known fact that the forward doubly virtual Compton scattering amplitude has a non-analytic behaviour in the real photon point $Q^2 = 0$, with Q^2 the virtuality of the incoming and outgoing photons. By now, it has been noticed for the low energy limit of the real and (doubly) virtual Compton scattering, where even the leading terms in the low energy expansion are sensitive to the order of taking either the low energy limit $\nu \to 0$ or $Q^2 \to 0$ first [15]. Our observation generalizes this non-analytical behaviour from the kinematical point $\nu = 0$, $t = 0$ to the whole forward axis $t = 0$.

The article is organized as follows: in Section II, we define the kinematics, general *ep*-scattering amplitude and the observables of interest; in Section III, the two photon exchange mechanism and the photons kinematics is studied; the equivalent photons or quasi real Compton scattering approximation and its implementation for the case of B_n is given in Section IV; we present our results in Section V which are followed up by a discussion and a summary.

II. ELASTIC *ep*-SCATTERING AMPLITUDE

In this work, we consider elastic electron-proton scattering process $e(k) + p(p) \to e(k') + p(p')$ for which we define:

$$\begin{aligned} P &= \frac{p+p'}{2} \\ K &= \frac{k+k'}{2} \\ q &= k - k' = p' - p, \end{aligned} \tag{1}$$

and choose the invariants $t = q^2 < 0$[2] and $\nu = (P\cdot K)/M$ as the independent variables. M denotes the nucleon mass. They are related to the Mandelstam variables $s = (p+k)^2$ and $u = (p-k')^2$ through $s - u = 4M\nu$ and $s + u + t = 2M^2$. For convenience, we also introduce the usual polarization parameter ε of the virtual photon, which can be related to the invariants ν and t (beglecting the electron mass m):

$$\varepsilon = \frac{\nu^2 - M^2\tau(1+\tau)}{\nu^2 + M^2\tau(1+\tau)}, \tag{2}$$

with $\tau = -t/(4M^2)$. Elastic scattering of two spin 1/2 particles is described by six independent amplitudes. Three of them do not flip the electron helicity [3],

$$\begin{aligned} T_{no\,flip} &= \frac{e^2}{-t}\bar{u}(k')\gamma_\mu u(k) \\ &\cdot\ \bar{u}(p')\left(\tilde{G}_M\gamma^\mu - \tilde{F}_2\frac{P^\mu}{M} + \tilde{F}_3\frac{\not{K}P^\mu}{M^2}\right)u(p), \end{aligned} \tag{3}$$

while the other three are electron helicity flipping and thus have in general the order of the electron mass m [13]:

$$\begin{aligned} T_{flip} &= \frac{m}{M}\frac{e^2}{-t}\left[\bar{u}(k')u(k)\cdot\bar{u}(p')\left(\tilde{F}_4 + \tilde{F}_5\frac{\not{K}}{M}\right)u(p)\right. \\ &\left. + \tilde{F}_6\bar{u}(k')\gamma_5 u(k)\cdot\bar{u}(p')\gamma_5 u(p)\right] \end{aligned} \tag{4}$$

In the one-photon exchange (Born) approximation, two of the six amplitudes match with the electromagnetic form factors,

$$\begin{aligned} \tilde{G}_M^{Born}(\nu,t) &= G_M(t), \\ \tilde{F}_2^{Born}(\nu,t) &= F_2(t), \\ \tilde{F}_{3,4,5,6}^{Born}(\nu,t) &= 0 \end{aligned} \tag{5}$$

where $G_M(t)$ and $F_2(t)$ are the magnetic and Pauli form factors, respectively. For further convenience we define also $\tilde{G}_E = \tilde{G}_M - (1+\tau)\tilde{F}_2$ and $\tilde{F}_1 = \tilde{G}_M - \tilde{F}_2$ which in the Born approximation reduce to electric form factor G_E and Dirac form factor F_1, respectively. For a beam polarized normal to the scattering plane, one can define a single spin asymmetry,

$$B_n = \frac{\sigma_\uparrow - \sigma_\downarrow}{\sigma_\uparrow + \sigma_\downarrow}, \tag{6}$$

where $\sigma_\uparrow$ ($\sigma_\downarrow$) denotes the cross sesction for an unpolarized target and for an electron beam spin parallel (antiparallel) to the normal polarization vector defined as

$$S_n^\mu = \left(0, \frac{[\vec{k}\times\vec{k'}]}{|\vec{k}\times\vec{k'}|}\right), \tag{7}$$

[2] In elastic *ep*-scattering, the usual notation for the momentum transfer is $Q^2 = -q^2$ but we prefer the more general notation t to avoid confusion with the incoming and outgoing photon virtualities in forward doubly virtual Compton scattering we will be concerned in the following.

normalized to $(S \cdot S) = -1$. Similarly, one defines the target normal spin asymmetry A_n. It has been shown in the early 1970's [7] that such asymmetries are directly related to the imaginary part of the T-matrix. Since the electromagnetic form factors and the one-photon exchange amplitude are purely real, B_n obtains its finite contribution to leading order in the electromagnetic constant α_{em} from an interference between the Born amplitude and the imaginary part of the two-photon exchange amplitude. In terms of the amplitudes of Eqs.(3,4), the beam normal spin asymmetry is given by:

$$B_n = -\frac{m}{M}\sqrt{2\varepsilon(1-\varepsilon)}\sqrt{1+\tau}\left(\tau G_M^2 + \varepsilon G_E^2\right)^{-1} \cdot \left\{\tau G_M \mathrm{Im}\tilde{F}_3 + G_E \mathrm{Im}\tilde{F}_4 + F_1 \frac{\nu}{M}\mathrm{Im}\tilde{F}_5\right\}. \quad (8)$$

For completeness, we also give here the expression of target normal spin asymmetry T_n [3] in terms of invariant amplitudes:

$$T_n = \sqrt{2\varepsilon(1+\varepsilon)}\sqrt{\tau}\left(\tau G_M^2 + \varepsilon G_E^2\right)^{-1} \cdot \left\{(1+\tau)\left[F_1 \mathrm{Im}\tilde{F}_2 - F_2 \mathrm{Im}\tilde{F}_1\right] + \left(\frac{2\varepsilon}{1+\varepsilon}G_E - G_M\right)\frac{\nu}{M}\mathrm{Im}\tilde{F}_3\right\}. \quad (9)$$

III. TWO PHOTON EXCHANGE

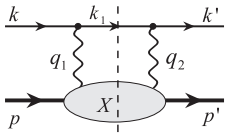

FIG. 1: Two-photon exchange diagram.

The imaginary part of the two-photon exchange (TPE) graph in Fig.1 is given by

$$\mathrm{Im}\mathcal{M}_{2\gamma} = e^2 \int \frac{|\vec{k}_1|^2 d|\vec{k}_1| d\Omega_{k_1}}{2E_1(2\pi)^3}\bar{u}'\gamma_\nu(\not{k}_1 + m)\gamma_\mu u \cdot \frac{1}{Q_1^2 Q_2^2}W^{\mu\nu}(w^2, Q_1^2, Q_2^2), \quad (10)$$

where $W^{\mu\nu}(w^2, Q_1^2, Q_2^2)$ is the imaginary part of doubly virtual Compton scattering tensor. Q_1^2 and Q_2^2 denote the virtualities of the exchanged photons in the TPE diagram, and w is the invariant mass of the intermediate hadronic system. We next study the kinematics of the exchanged photons. Neglecting the small electron mass and using the c.m. frame of the electron and proton, one has:

$$Q_{1,2}^2 = 2|\vec{k}||\vec{k}_1|(1 - \cos\Theta_{1,2}), \quad (11)$$

with $|\vec{k}| = \frac{s-M^2}{2\sqrt{s}} \equiv k$ the three momentum of the incoming (and outgoing) eletron, $|\vec{k}_1| = \sqrt{(\frac{s-w^2+m^2}{2\sqrt{s}})^2 - m^2}$ that of the intermediate electron, and $\cos\Theta_2 = \cos\Theta\cos\Theta_1 + \sin\Theta\sin\Theta_1\cos\phi$. The kinematically allowed values of the virtualities of the exchanged photons (the restriction is due to the fact that the intermediate electron is on-shell) are represented by the internal area of the ellypses shown in Fig. 2. The ellypses are drawn

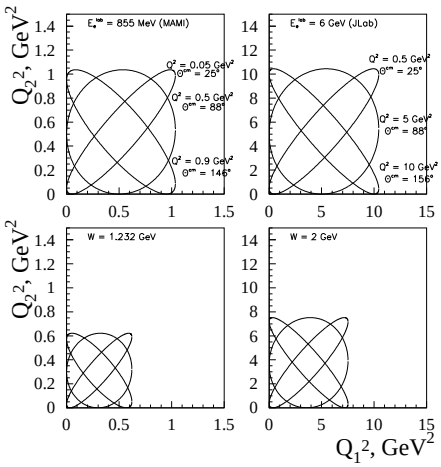

FIG. 2: Kinematically allowed values of the photon vitualities $Q_{1,2}^2$.

inside a square whose side is defined through the external kinematics (k) and the invariant mass of the intermediate hadronic state (w^2 or k_1), while the form solely by the scattering angle. If choosing higher values of the mass of the hadronic system $w^2 < s$, it leads to scaling the size of the ellypse by a factor of $\frac{s-w^2}{s-M^2}$. In the limit $w^2 = (\sqrt{s} - m_e)^2$, the ellypses shrink to a point at the origin and both photons are nearly real. This is not a collinear singularity, however, since the real photons' energy remains large enough in order to provide the transition from nucleon with the mass M to the intermediate state X with the mass w. Instead, the intermediate electron is soft, $k_1^\mu \approx (m_e, \vec{0})$, therefore this kind of kinematics does not lead to an IR divergency which can only occur if the intermediate hadronic state is the nucleon itself. In the following we are going to study this kinematical situation in more detail.

IV. QUASI-RCS APPROXIMATION

We consider the kinematical factors under the integral over the electron phase space of Eq.(10) at the upper

[3] Also A_n notation for target normal spin asymmetry exists in the literature.

limit of the integration over the invariant mass of the intermediate hadronic state, $w \to \sqrt{s} - m_e$:

$$\frac{\vec{k}_1^2}{E_1}\frac{1}{Q_1^2 Q_2^2} \sim \frac{1}{4k^2 E_1} \sim \frac{1}{m}\frac{1}{4k^2}, \tag{12}$$

In this range of the hadronic mass w, the exchanged photons are real, and the contribution of real Compton scattering (RCS) to the 2γ-exchange graph is enhanced by a factor of $1/m$ (it is not a singularity since B_n has a factor of m in front). This enhancement, however, only appears for the beam asymmetry B_n since the target asymmetry does not involve the electron spin flip and the electron mass can be neglected in the electron propagator $\not{k}_1 + m$ in the numerator of Eq.(10). The remaining $\not{k}_1$ cancels this $1/m$ behaviour.

We next rewrite the hadronic tensor in Eq.(10) identically as

$$\begin{aligned} W^{\mu\nu}(W^2, Q_1^2, Q_2^2) &= W^{\mu\nu}(s, 0, 0) \\ &+ (W^{\mu\nu}(W^2, Q_1^2, Q_2^2) - W^{\mu\nu}(s, 0, 0)), \end{aligned} \tag{13}$$

so that only the first term is now enhanced in this limit, while the second term vanishes at the RCS point by construction. Equivalent photon or quasi-real Compton scattering (QRCS) approximation consists in assuming the first term to be dominant due to the kinematical enhancement under the integral and in neglecting the second one. The question of the validity of such an approximation should be raised for the beam normal spin asymmetry. We will come back to this point in Section V. However, in general, this kind of contributions coming from QRCS kinematics will allways be present in the full calculation, since the second term in Eq.(14) is constructed in such a way that the resulting integral is regular at the QRCS point. In the following, the QRCS approximation will be used. Hence, the hadronic tensor can be taken out of the integration over the electron phase space. The remaining integrals are

$$\begin{aligned} I_0 &= \int \frac{d^3\vec{k}_1}{2E_1(2\pi)^3}\frac{1}{Q_1^2 Q_2^2} \\ I_1^\mu &= \int \frac{d^3\vec{k}_1}{2E_1(2\pi)^3}\frac{k_1^\mu}{Q_1^2 Q_2^2} = K^\mu I_{1K} + P^\mu I_{1P}, \end{aligned} \tag{14}$$

We next list the result of the integration in the limit of high energies (i.e., neglecting terms $\sim m_\pi/E$):

$$\begin{aligned} I_0 &= \frac{1}{-32\pi^2 t}\left[\ln^2\left(\frac{-t}{m^2}\right) + 4\frac{\pi^2}{3}\right], \\ I_{1P} &= \frac{1}{16\pi^2}\frac{s-M^2}{M^4 - su}\ln\left(\frac{4E^2}{-t}\right), \\ I_{1K} &= \frac{1}{-4\pi^2 t}\ln\left(\frac{2E}{m}\right) + \frac{4M\nu}{t}I_{1P} \\ &\equiv I_{1K}^0 + \frac{4M\nu}{t}I_{1P}. \end{aligned} \tag{15}$$

For the details, we address the reader to the Appendix. The three integrals I_0, I_{1K}^0, and I_{1P} obviously classify as $\log^2 m$, $\log^1 m$, and $\log^0 m$, respectively. In Ref. [14] only the first integral was calculated.

The RCS tensor may be taken for instance in the basis of Prange [16] or, equivalently of Berg and Lindner [17],

$$\begin{aligned} W_{RCS}^{\mu\nu} &= \bar{N}'\left\{\frac{P'^\mu P'^\nu}{P'^2}(B_1 + \not{K}B_2) + \frac{n^\mu n^\nu}{n^2}(B_3 + \not{K}B_4)\right. \\ &+ \frac{P'^\mu n^\nu - n^\mu P'^\nu}{P'^2 n^2}\, i\gamma_5 B_7 \\ &\left. + \frac{P'^\mu n^\nu + n^\mu P'^\nu}{P'^2 n^2}\not{n}B_6\right\} N, \end{aligned} \tag{16}$$

with the vectors defined as $P' = P - \frac{P\cdot K}{K^2}K$, $n^\mu = \varepsilon^{\mu\nu\alpha\beta}P_\nu K_\alpha q_\beta$ such that $P'\cdot K = P'\cdot n = n\cdot K = 0$. The amplitudes B_i are functions of ν and t. This form of Compton tensor is convenient due to the simple form of the tensors appearing in Eq. (16). However, the amplitudes B_i possess kinematical singularities and constraints, therefore in the following we will also use another set of invariant amplitudes introduced as combinations of B_i's in [18]. This latter set of amplitudes is widely used in the dispersion analysis of Compton experiments, high energy contributions to them are well studied, and we will take an advantage of this knowledge.

Before contracting the leptonic and hadronic tensors, we notice that the amplitude B_7 can only contribute to the invariant amplitude $\tilde{F}_6$, since it contains the $\bar{N}'\gamma_5 N$ structure. $\tilde{F}_6$ does not contribute at leading order in m to neither obserevable of interest, therefore B_7 will be neglected in the following. The remaining tensors in Eq.(16) are symmetric in indices $\mu\nu$.

$$\begin{aligned} \mathrm{Im}\mathcal{M}_{2\gamma}^{QRCS} &= e^2\bar{u}'\gamma_\nu(\not{I}_1 + mI_0)\gamma_\mu u W_{RCS}^{\mu\nu} \\ &= \bar{u}'(-\not{I}_1 + mI_0)u W_{RCS}^{\mu\nu}g_{\mu\nu} \\ &+ 2W_{RCS}^{\mu\nu}I_{1\mu}\bar{u}'\gamma_\nu u. \end{aligned} \tag{17}$$

Finally, we identify different terms in Eq. (17) with the structures, together with amplitudes $\tilde{F}_{1,\dots 6}$ parametrizing elastic ep-scattering amplitude in Eqs. (3,4) and after some algebra we find for the invariant amplitudes for the elastic electron-proton scattering in the QRCS approximation:

$$\mathrm{Im}\tilde{G}_M^{QRCS} = -2tI_{1P}\mathrm{Im}B_6 \tag{18}$$

$$\begin{aligned} \mathrm{Im}\tilde{F}_2^{QRCS} &= -MtI_{1P} \\ &\cdot\ \mathrm{Im}\left[B_1 - B_3 - \frac{2Mt}{M^4 - su}B_6\right] \end{aligned} \tag{19}$$

$$\begin{aligned} \mathrm{Im}\tilde{F}_3^{QRCS} &= -M^2 tI_{1P}\mathrm{Im} \\ &\cdot\ \mathrm{Im}\left[B_2 - B_4 - \frac{8M\nu}{M^4 - su}B_6\right], \end{aligned} \tag{20}$$

$$\begin{aligned}
\mathrm{Im}\tilde{F}_4^{QRCS} &= -Mt(I_0 - I_{1K})\mathrm{Im}(B_1 + B_3) \\
&- 4M^2\nu I_{1P}\Big[\mathrm{Im}(B_1 - B_3) \\
&\quad - \frac{2Mt}{M^4 - su}\mathrm{Im}B_6\Big] \qquad (21) \\
\mathrm{Im}\tilde{F}_5^{QRCS} &= -M^2t(I_0 - I_{1K})\mathrm{Im}(B_2 + B_4) \\
&- 4M^3\nu I_{1P}\mathrm{Im}(B_2 - B_4) \\
&- \frac{2M^2t(4M^2 - t)}{M^4 - su}\mathrm{Im}B_6 \qquad (22)
\end{aligned}$$

We use next the forward kinematics and obtain for B_n in the QRCS approximation:

$$\begin{aligned}
B_n^{QRCS} &= \frac{m}{M}\frac{\sqrt{-t}}{\nu}\frac{F_1}{F_1^2 + \tau F_2^2} \\
&\cdot \{Mt(I_0 - I_{1K})\mathrm{Im}\left[B1 + B_3 + \nu(B_2 + B_4)\right] \\
&\quad + 4M^2\nu I_{1P}\mathrm{Im}\left[B1 - B_3 + \nu(B_2 - B_4)\right]\} \\
&= -\frac{m}{M}\frac{\sqrt{-t}}{\nu}\frac{F_1}{F_1^2 + \tau F_2^2} \\
&\cdot \left\{Mt^2(I_0 - I_{1K})\mathrm{Im}A_1\right. \\
&\quad \left. + 4M^2\nu I_{1P}4\nu^2\mathrm{Im}(A_3 + A_6)\right\}, \qquad (23)
\end{aligned}$$

where the invariant amplitudes of Lvov [18] are used instead of combinations of B_i appearing in the result. We make use of the well known physics content of the amplitudes A_1 and $A_3 + A_6$ entering the final result of Eq.(23). In terms of the helicity amplitudes of real Compton scattering defined as $T_{\lambda'_\gamma\lambda'_N,\lambda_\gamma\lambda_N} \equiv \varepsilon^{\prime *\nu}_{\lambda'_\gamma}\varepsilon^{\mu}_{\lambda'_\gamma}W^{RCS}_{\mu\nu}$, one has [18]:

$$\begin{aligned}
A_1 &= \frac{s - M^2}{MQ^2\sqrt{M^4 - su}}T_{1\frac{1}{2},-1\frac{1}{2}} \qquad (24) \\
&+ \frac{1}{2\sqrt{Q^2}(s - M^2)}\left(T_{-1-\frac{1}{2},1\frac{1}{2}} + T_{1-\frac{1}{2},-1\frac{1}{2}}\right), \\
A_3 + A_6 &= \frac{1}{4\nu\sqrt{M^4 - su}}\left(T_{1\frac{1}{2},1\frac{1}{2}} + T_{1\frac{1}{2},1\frac{1}{2}}\right), \qquad (25)
\end{aligned}$$

It can be seen that the combination $A_3 + A_6$ involves only helicity amplitudes without helicity flip, while A_1 does flip photon helicity. Basing on the analysis of RCS [18], we know furthermore that the real part of $\mathrm{Re}(A_3 + A_6)$ is related to the forward nucleon polarizability $(\alpha + \beta)$, while $\mathrm{Re}A_1$ is related to the backward polarizability $(\alpha - \beta)$. It is interesting to observe that the backward RCS physics enters the expressions for forward *ep*-scattering amplitudes. This result is in fact model independent, since the contribution from the QRCS peak is always present in the full result. The role of the QRCS approximation used here is in neglection of the other contributions which might obscure this important observation. Moreover, we see in Eq.(23) that the forward combination of the RCS amplitudes enters B_n multyplied by the integral I_{1P} which is peaked in the forward direction, as well, and the backward combinations with the backward peaked integrals $I_0 - I_{1K}$. This result is in disagreement with the result of Ref. [14], where the *ep*-scattering amplitude in the forward direction is parametrized through the total photoabsorption cross section and the backward integral I_0. This discrepancy will be discussed in more detail in Section VI.

In the following, we use the total photoabsorption cross section as the phenomenological input to $\mathrm{Im}(A_3 + A_6)$ in the forward regime [18]

$$\mathrm{Im}(A_3 + A_6)(s, t = 0) = -\frac{1}{2\nu}\sigma^{tot}_{\gamma N}\left(\frac{s}{s_0}\right)^{\alpha_P(0)-1} \qquad (26)$$

with the total photoabsorption cross section $\sigma^{tot}_{\gamma N} \approx 0.1$ mbarn. Furthermore, we adopted the standard Regge behaviour in order to assure a correct energy dependence with the pomeron intercept $\alpha_P(0) = 1.08$ and the parameter $s_0 = 1$ GeV. For t dependence, we use an exponential suppression factor $\exp(Bt/2)$ with $B = 8$ GeV^{-2}, which provides a good description of Compton cross section for $-t \leq 0.8$ GeV^2 [22].

The amplitude A_1 in Regge regime is known to have the quantum numbers of a scalar isoscalar exchange in the t-channel which was successfully described by σ-meson [18] or equivalently, by two pion exchange in the t-channel [19]. Since the effective σ-meson exchange does not result in a non-zero imaginary part in the s-channel, one should use the two pion exchange mechanism accompanied by multiparticle intermediate state in the s-channel. In this work we estimate A_1 through πN and ρN contributions within the "minimal" Regge model for π and ρ photoproduction [23] where reggeized description of high energy pion production is obtained by adding the t-channel meson exchange amplitude and (in the case of γp reaction) s-channel Born amplitude which is necessary to ensure gauge invariance. The reggeization procedure naturally leads to the substitution of each t-channel Feynman propagator by its Regge counterpart, $\frac{1}{t-m_\pi^2} \to \mathcal{P}_\pi^R(\alpha_\pi(t))$, with

$$\mathcal{P}_R^\pi = \left(\frac{s}{s_0}\right)^{\alpha_\pi(t)}\frac{\pi\alpha'_\pi}{\sin\pi\alpha_\pi(t)}\frac{1}{\Gamma(1 + \alpha_\pi(t))}, \qquad (27)$$

with $\alpha_\pi(t) = \alpha'_\pi(t - m_\pi^2)$ and $\alpha'_\pi = 0.7$ GeV^{-2}. Gauge invariance requires the s-channel piece to be reggeized in the same way, i.e., to be multiplied by $(t - m_\pi^2)\mathcal{P}_\pi^R(\alpha_\pi(t))$. Here we list the results of the calculation of A_1:

$$\begin{aligned}
\mathrm{Im}A_1^{\pi N} &= \frac{2m_\pi^2 C_\pi^2}{M(s - M^2)}(B_0^\pi - M^2A_0^\pi), \qquad (28) \\
\mathrm{Im}A_1^{\rho N} &= \frac{m_\rho^2 C_\rho^2}{2M(s - M^2)}\left\{\frac{M^2}{s - M^2}C_0^\rho\right. \\
&\quad \left. + \frac{s - 3M^2 + 5m_\rho^2}{2}B_0^\rho + m_\rho^2\frac{s + M^2}{2}A_0^\rho\right\},
\end{aligned}$$

where $C_\pi = 2\sqrt{2}Me\frac{f_{\pi NN}}{m_\pi}$ with $f^2_{\pi NN}/4\pi = 0.08$, and $C_\rho = 2\sqrt{2}Me\frac{f_{\rho NN}}{m_\pi}\frac{f_{\rho\pi\gamma}}{m_\pi}$ with $f_{\rho\pi\gamma} = 0.103$ [23]. Where

possible, m_π and Q^2 were neglected as compared to s, M, m_ρ in order to simplify the final expression. The scalar integrals A_0, B_0, C_0 for both πN and ρN contributions are given in the Appendix. In Fig. 3, we show the ratio of the reggeized version of the integrals $(A, B, C)^\rho$ and the analytic results. The amplitude A_1 is defined as the

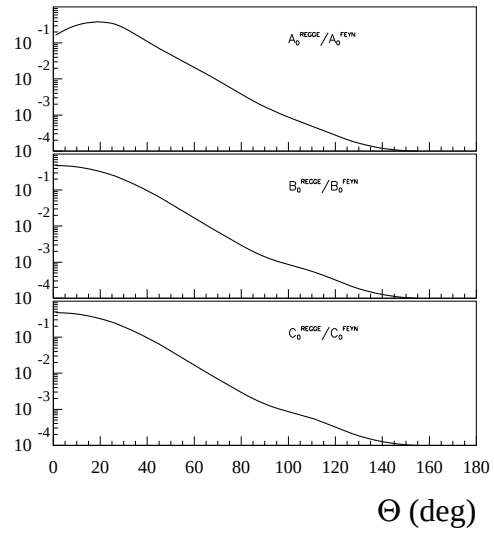

FIG. 3: Ratio of the integrals with Regge propagators in the t-channel to the analytic results with pion Feynman propagators is shown for A_0^ρ (upper panel), B_0^ρ (upper panel), C_0^ρ (upper panel) as function of c.m. scattering angle for beam energy $E_{lab} = 5.77$ GeV.

combination $\frac{1}{-t}[B_1+B_3+\nu(B_2+B_4)]$, and the singularity $\frac{1}{t}$ in the definition only cancels if taking the gauge invariant combination as described in [23]. The other feature of the result of Eqs.(28,29) is that both contributions are suppressed by factors $\frac{m_\pi^2}{s-M^2}$ and $\frac{m_\rho^2}{s-M^2}$, respectivelyly. In the case of the pion, it is interesting to observe this fact in view of somewhat surprising success of the effective field description of the SAMPLE data point on B_n without pion contribution. This might give a hint that the pion contribution to B_n at low energies is suppressed by the pion mass, if calculated to the same order.

V. RESULTS

We now present the results for B_n using the model described in the previous section. In Fig. 4, beam normal spin asymmetry for the proton target is shown as function of Q^2 for four different values of *lab* electron beam energy. In Fig. 4, the sum of forward $A_3 + A_6 \sim \sigma_{tot}$ and backward $A_1 \sim \pi\pi$-exchange is shown. However, the impact of the latter is negligibly small in the kinematics shown and is far below 1% for all energies considered. The reason for that are the both suppression factors $\frac{m_{\pi,\rho}}{(s-M^2)}$ and $\frac{Q_2}{(s-M^2)}$ together with the Regge suppression due to the pion trajectory, as compared to the Pomeron.

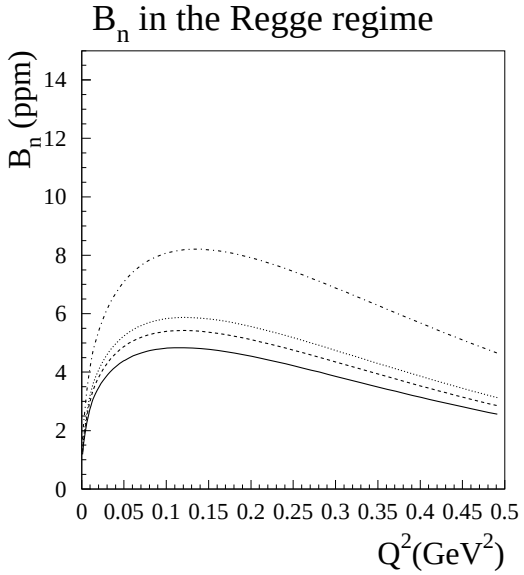

FIG. 4: Results for B_n as function of Q^2 for different values of the LAB energy of the electron: 6 GeV (solid line), 9 GeV (dashed line), 12 GeV (dotted line) and 45 GeV (dashed-dotted line).

So, the $\log^2 m$ enhancement of B_n is absolutely irrelevant in this extreme forward kinematics. Recalling that this $\log^2 m$ term factorizes the backward Compton amplitude contribution, this is by no means a surprise, since it is unphysical for bacward mechanisms to dominate forward observables. This result suggests in turn that the QRCS approximation should not be expected to work in the forward kinematics. In fact, this effect was observed on the example of πN intermediate state contribution in [10]. However, if going to backward angles, this contribution increases as $\sim |t| \ln^2(|t|/m^2)$ and, in general, the approximation is justified. In the forward kinematics, the energy dependence in Eq.(23) originates thus mostly from the term $\ln \frac{2E}{\sqrt{|t|}}$, so that the asymmetry increases logarithmically with the energy. This is an interesting observation and is on contrary with the dominant energy dependence of B_n at low energies where it decreases with energy as m/E. It furthermore gives good outlook for measuring B_n through high energy region at forward angles. Still, a full calculation (beyond the QRCS approximation) is needed to confirm this behaviour. Comparing to the calculation of [14], the quite different way the real Compton scattering amplitudes enter the final result for B_n leads to inversed energy dependence and consequently, the largest disagreement between the two calculations amounts in an order of magnitude for the JLab energy, lowest among those considered. This discrepancy will be discussed in details in the next section.

VI. DISCUSSION

As it has been noticed before, the presented calculation is in disagreement with the result of Ref. [14]. Their approach consisted in taking only the part of doubly virtual Compton tensor which survives in the exact forward limit of real Compton scattering (see Eq. (14) of [14])

$$M^{\mu\nu} = \left\{-(PK)^2 g^{\mu\nu} - (q_1 q_2) P^\mu P^\nu + (PK)\left[P^\mu q_1^\nu + P^\nu q_2^\mu\right]\right\}\mathcal{A}, \quad (29)$$

with $\mathcal{A}$ the forward amplitude of doubly virtual Compton scattering which is then related to the proton structure function F_1 and the total photoabsorption cross section $\sigma_{\gamma p}^{tot}$. The forward spin independent doubly virtual Compton scattering tensor is usually written in terms of the DIS structure functions W_1, W_2,

$$\begin{aligned} W^{\mu\nu} &= O_1^{\mu\nu} W_1(\nu, Q^2) + O_2^{\mu\nu} W_2(\nu, Q^2) \\ &= \left(-g^{\mu\nu} + \frac{q_2^\mu q_1^\nu}{(q_1 \cdot q_2)}\right) W_1 \\ &+ \frac{1}{M\nu}\left(P^\mu + \frac{Pq_1}{(q_1 \cdot q_2)} q_2^\mu\right)\left(P^\nu + \frac{Pq_2}{(q_1 \cdot q_2)} q_1^\nu\right) W_2, \end{aligned} \quad (30)$$

where the tensors should be taken in the limit $q_1 = q_2$. In the scaling limit, one has $W_1(\nu, Q^2) \to F_1(x)$, $W_2(\nu, Q^2) \to F_2(x)$, and the Callan-Gross relation implies $F_2 = 2xF_1$. We rewrite now the tensor of Eq.(30) in terms of the DIS tensors $O_1^{\mu\nu}, O_2^{\mu\nu}$:

$$M^{\mu\nu} = (PK)^2 \left\{O_1^{\mu\nu} - \frac{q_1 \cdot q_2}{P \cdot K} O_2^{\mu\nu}\right\}\mathcal{A}. \quad (31)$$

We proceed by projecting this tensor onto the basis of Prange, make use of $\frac{q_1 \cdot q_2}{K^2} = 2 + \frac{Q_1^2 + Q_2^2}{2K^2}$, and obtain for the amplitudes' combination which multiplies the $\ln^2 m$ term:

$$B_1 + B_2 + \nu(B_2 + B_4) = \frac{(PK)^2}{2M}\frac{Q_1^2 + Q_2^2}{2K^2}\mathcal{A}, \quad (32)$$

The kinematical limit of Ref. [14] corresponds to neglecting t comparing to the photons' virtualities. Then, $q_1 = q_2 = K$, and the right hand side is non-zero. Instead, throughout this work, the non-forward RCS kinematics with the on-shell photons is used, and the contribution of the cross section (i.e., helicity conserving helicity amplitudes) to Eq.(32) vanishes. It is an interesting phenomenon, that the result of taking the limit $Q_{1,2}^2 \to 0$ and $t \to 0$ is order depending.

The dependence on the order of taking the limit $Q^2 \to 0$ and low photon energy limit has been observed before in the context of polarizabilities of RCS and generalized polarizabilities of VCS [24], and even for the leading term in photon energy of the forward RCS vs. forward doubly VCS amplitude $F(\nu, Q^2)$ [15]:

$$\begin{aligned} \lim_{\nu\to 0}\lim_{Q^2\to 0} F(\nu, Q^2) &= -\frac{\alpha_{em}}{M} e_N (\vec{\varepsilon}'^* \cdot \vec{\varepsilon}), \\ \lim_{Q^2\to 0}\lim_{\nu\to 0} F(\nu, Q^2) &= \frac{\alpha_{em}}{M}\kappa_N(2e_N + \kappa_N)(\vec{\varepsilon}'^* \cdot \vec{\varepsilon}), \end{aligned} \quad (33)$$

with e_N and κ_N the charge and the a.m.m. of the nucleon (1 and 1.79 for the proton and 0 and -1.91 for the neutron, respectively). So, it is not completely unexpected that the two different limits do not match. In Fig. 5,

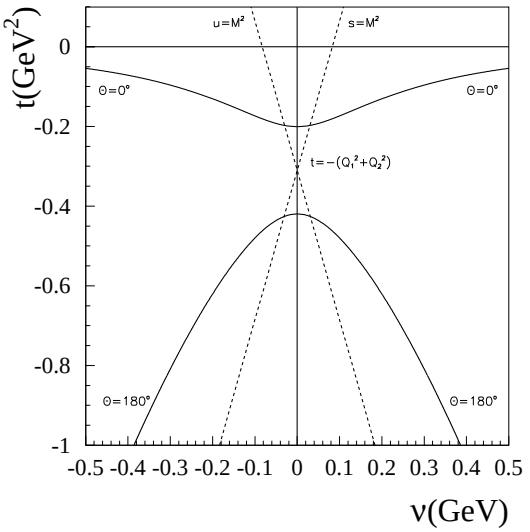

FIG. 5: Mandelstam plot for doubly virtual Compton scattering with $Q_1^2 = 0.3$ GeV^2 and $Q_2^2 = 0.01$ GeV^2. For further details, see text.

the Mandelstam plot for the general case of doubly virtual Compton scattering is shown for $Q_1^2 = 0.3$ GeV^2 and $Q_2^2 = 0.01$ GeV^2. The plot shows different kinematical regions on the plane $\nu = \frac{Pq_1}{M}$ and t. The energy threshold for the reaction in the s-channel, $s = M^2$, is represented by the straight line $\nu = \frac{t+Q_1^2+Q_2^2}{4M}$, so that the s-channel reaction (direct Compton scattering) is possible to the right of this line. The requirement that the scattering angle takes physical values, restricts allowed values for the variables ν and t to the area between the two curves depicted in the right half-plane. The upper line corresponds to $\cos\Theta = 1$ (forward scattering), while the lower one ot $\cos\Theta = -1$ (backward scattering). The physical scattering can only occur inside this region. The forward line crosses the t axis at $t = -(\sqrt{Q_1^2} - \sqrt{Q_2^2})^2$, while the backward line at $t = -(\sqrt{Q_1^2} + \sqrt{Q_2^2})^2$. The u-channel (crossed Compton reaction) kinematical regions are obtaine by $\nu \to -\nu$. The variable ν should not be confused with the energy of the virtual photon, which is sometimes denoted as ν, as well. In the lab frame, the initial photon energy is given by $\omega_1 = \frac{w^2 - M^2 + Q_1^2}{2M}$, while $\nu = \frac{2(w^2 - M^2) + t + Q_1^2 + Q_2^2}{4M}$, with $w^2 = (p + q_1)^2$ the invariant mass squared of the intermediate hadronic state. For each value of the external variables s and t which one measures in a ep-scattering experiment, the integral over the intermediate electron phase space involves $\int_{M^2}^{(\sqrt{s}-m)^2} dw^2$ and $\int dQ_1^2 dQ_2^2$. The latter integral is performed over the ellyptic areas shown in Fig. 2, unambiguously defined by s, t and w^2. In terms of the Mandelstam plot in Fig. 5, this corresponds to integrating over a se-

ries of such Mandelstam plots for each pair of Q_1^2, Q_2^2 at the value of t fixed by the experimental kinematics. In the special case of $Q_1^2 = Q_2^2$ which is always contained within the integral, as can be seen in Fig. 2, the Mandelstam plot is deformed, so that the forward line becomes $t = 0$. If $Q_1^2 \neq Q_2^2$, however, $t = 0$ is only approached asymptotically for $\nu \to \infty$. This is the reason why the limit $t \to 0$ is not well defined for the general case of the doubly virtual Compton scattering: this limit takes one outside of the physical region of the reaction. If one preforms the limit $Q_{1,2}^2 \to 0$ first, keeping $t \neq 0$, one enssures that the line $t = 0$ is contained within the physical region, and the limit can be performed.

Technically, the difference between the two limits originates from treating as small quantity either the momentum transfer (forward doubly VCS) or the virtualities of the photons (RCS). We note that the squared logarithm enhancement occurs if the hadronic amplitudes is nonzero in the exact limit of hard collinear photons. Therefore, the leading (in $\log^2 m$) contribution should correspond to Compton scattering with the photon virtualities of the order $Q_1^2 = -(k - k_1)^2 \approx 2mE$ and the momentum transfer of the ep reaction which one measures on the experiment. It means that in order to justify the limit of [14], one has to go to external momentum transfers smaller than $2mE$ which is of the order of 10^{-3} GeV^2 in the kinematics considered here. Apart from difficulty in achieving this kinematics experimentally, it is suppressed by the kinematical factors in the general expression of Eq.(8)for B_n, which ensures this observable to vanish in the exact forward direction. Basing on these considerations, we see that in order to obtain adequate estimate of the double log effect for B_n, one has to split the full doubly virtual Compton amplitude into the non-forward real Compton amplitude which gives the desirable effect, plus the rest which is regular in the QRCS point and can at most give a $\ln m$ effect.

VII. SUMMARY

In summary, we presented a calculation of the beam normal spin asymmetry in the kinematical regime of high energies ($E_{lab} = 6-45$ GeV) and low momentum transfer to the target, $Q^2 \leq 0.5$ (GeV/c)^2. This observable obtains its leading contribution from the imaginary part of the two photon exchange graph times the Born amplitude and is directly related to the imaginary part of doubly virtual Compton scattering The resulting loop integral obtains a large contribution from the kinematics when both exchanged photons are nearly real and collinear to the external electrons. We adopt the QRCS or equivalent photons approximation which allows to take the hadronic part in the external kinematics out of the integral and to perform the integration over the electron phase space analytically. For the hadronic part, we use the full real Compton scattering amplitude and show, that both forward (no proton and photon helicity flip) and backward (photon helicity flipping) amplitudes do contribute in this observable in the forward kinematics. For the forward Compton amplitude, we use optical theorem as the input. For backward Compton amplitude, we provide an explicite calculation which is due to two pion exchange in the t-channel. The resulting values of the asymmetry are in the range $4 - 8$ ppm for the energies in the range $6 - 45$ GeV. We find furthermore that the double logarithmic enhancement does not dominate B_n in forward regime since it comes with helicity-flip Compton amplitude which highly suppresses this behaviour. Finally, we make an interesting observation that the non-analyticity of the doubly virtual Compton scattering leads to the order dependence of taking limits $t \to 0$ and $Q_{1,2}^2 \to 0$, which is a generalization of the known problem of matching the low energy limits of real and doubly virtual Compton scattering.

Acknowledgments

The author is grateful to Prof. M.M.Giannini for continuous support and to Dr. M.J. Ramsey-Musolf and Dr. V. Cirigliano for numerous discussions and for thorough reading of the manuscript. The work was supported by Italian MIUR and INFN, and by US Department of Energy Contract DE-FG02-05ER41361.

VIII. APPENDIX A: INTEGRALS OVER ELECTRON PHASE SPACE

In this section we present calculation of the integrals over electron phase space appearing in the QRCS approximation. First we calculate the scalar integral I_0,

$$I_0 = \int_0^{k_{thr}} \frac{k_1^2 dk_1}{2E_1(2\pi^3)} \int \frac{d\Omega_{k_1}}{(k-k_1)^2(k'-k_1)^2}, \quad (34)$$

where the upper integration limit k_{thr} corresponds to the inelastic threshold (i.e. pion production), $k_{thr} = \sqrt{\frac{(s-(M+m_pi)^2)^2}{4s} - m^2}$. We next introduce integration over the Feynman parameter $\frac{1}{ab} = \int_0^1 \frac{dx}{[a+(b-a)x]^2}$. We chose the polar axis such as $\vec{k}_1 \cdot (\vec{k} - x\vec{q}) = k_1 |\vec{k} - x\vec{q}| \cos\Theta_1$ with $|\vec{k} - x\vec{q}|^2 = k^2 + x(1-x)t$ and perform angular integration. We furthermore change integration over dk_1 to integration over dimensionsless $z = E_1/E$

$$I_0 = \frac{1}{-8\pi^2 t} \int_{\frac{m}{E}}^{\frac{E_{thr}}{E}} \frac{dz}{\sqrt{z^2 - \frac{m^2}{E^2} - \frac{4m^2}{t}(1-z)^2}} \cdot \ln \frac{\sqrt{z^2 - \frac{m^2}{E^2} - \frac{4m^2}{t}(1-z)^2} + \sqrt{z^2 - \frac{m^2}{E^2}}}{\sqrt{z^2 - \frac{m^2}{E^2} - \frac{4m^2}{t}(1-z)^2} - \sqrt{z^2 - \frac{m^2}{E^2}}}, \quad (35)$$

To perform the integration over the electron energy, we follow here the main details of the calculation in Ap-

pendix A of Ref.[14]. The result reads

$$I_0 \;=\; \frac{1}{-32\pi^2}\left\{\ln^2\left(\frac{-t}{m^2}\frac{E_{thr}^2}{E^2}\right) \;+\; 8Sp\left(\frac{E_{thr}}{E}\right)\right\}, \quad (36)$$

where $Sp(x)$ is the Spence or dilog function, $Sp(x) = -\int_0^1 \frac{dt}{t}\ln(1-xt)$ with $Sp(1) = \pi^2/6$. In the high energy limit, $\frac{E_{thr}}{E} \to 1$, we recover the result of Ref.[14].

We next turn to the vector integral

$$\begin{aligned} I_1^\mu \;&=\; \int_0^{k_{thr}} \frac{k_1^2 dk_1}{2E_1(2\pi^3)} \int d\Omega_{k_1} \frac{k_1^\mu}{(k-k_1)^2(k'-k_1)^2} \\ &=\; I_{1P}P^\mu \;+\; I_{1K}K^\mu\,. \end{aligned} \quad (37)$$

It cannot depend on q^μ due to the symmetry of I_1 under interchanging k and k'. To determine these two coefficients we have a system of equations,

$$\begin{aligned} K^0 I_{1K} \;+\; P^0 I_{1P} \;&=\; I_1^0 \;=\; \frac{1}{16\pi^3}\int \frac{d^3\vec{k}_1}{Q_1^2 Q_2^2} \quad (38)\\ -tI_{1K} \;+\; 4PKI_{1P} \;&=\; 4K_\mu I_1^\mu \;=\; \int \frac{d^3\vec{k}_1}{(2\pi^3)E_1 Q_1^2} \\ &\equiv\; I_2. \end{aligned}$$

Using the same approach as for I_0, we obtain for I_1^0:

$$\begin{aligned} I_1^0 \;&=\; \frac{E}{-8\pi^2 t}\int_{\frac{m}{E}}^{\frac{E_{thr}}{E}} \frac{z dz}{\sqrt{z^2 - \frac{m^2}{E^2} - \frac{4m^2}{t}(1-z)^2}} \quad (39)\\ &\qquad \cdot \ln \frac{\sqrt{z^2 - \frac{m^2}{E^2} - \frac{4m^2}{t}(1-z)^2} + \sqrt{z^2 - \frac{m^2}{E^2}}}{\sqrt{z^2 - \frac{m^2}{E^2} - \frac{4m^2}{t}(1-z)^2} - \sqrt{z^2 - \frac{m^2}{E^2}}} \\ &=\; \frac{E}{-4\pi^2 t}\left\{\frac{E_{thr}}{E}\ln\frac{\sqrt{-t}}{m}\frac{E_{thr}}{E}\right. \quad (40)\\ &\qquad \left. +\left(1-\frac{E_{thr}}{E}\right)\ln\left(1-\frac{E_{thr}}{E}\right)\right\}. \quad (41) \end{aligned}$$

Finally, we consider the integral I_2 where we perform angular integration,

$$\begin{aligned} I_2 \;&=\; \frac{1}{(2\pi^3)}\int \frac{d^3\vec{k}_1}{E_1 Q_1^2} \quad (42)\\ &=\; \pi\int_{\frac{m}{E}}^{\frac{E_{thr}}{E}} dz \ln \frac{z - \frac{m^2}{E^2} + \sqrt{1-\frac{m^2}{E^2}}\sqrt{z^2-\frac{m^2}{E^2}}}{z - \frac{m^2}{E^2} - \sqrt{1-\frac{m^2}{E^2}}\sqrt{z^2-\frac{m^2}{E^2}}}. \end{aligned}$$

After integrating by parts and changing variables consequently $z = \frac{m}{E}\cosh y$ and $y = \ln t$, we arrive to

$$\begin{aligned} I_2 \;&=\; 2\pi\frac{E_{thr}}{E}\ln\frac{2E_{thr}}{m} \quad (43)\\ &\quad +\; 2\pi\left(1-\frac{E_{thr}}{E}\right)\ln\left(1-\frac{E_{thr}}{E}\right). \end{aligned}$$

In these last two integrals, it is important to keep $\frac{E_{thr}}{E}$ unequal to 1 till the end to ensure the convergence of the integral. Solving the system of linear equations for the coefficients, we obtain:

$$\begin{aligned} I_{1P} \;&=\; \pi\frac{s-M^2}{M^4-su}\frac{E_{thr}}{E}\ln\frac{2E}{Q} \\ I_{1K} \;&=\; \frac{1}{Q^2}I_2 - \frac{4PK}{Q^2}I_{1P}. \end{aligned} \quad (44)$$

IX. APPENDIX B: SCALAR INTEGRALS FOR HELICITY FLIP AMPLITUDE

The vector and tensor integrals can be reduced to the scalar ones by means of standard methods [25]. The remaining integrals to be calculated are the two, three, and four-point scalar integrals. Here we are only interested in the imaginary part of these, therefore there are only three integrals with non-zero imaginary part: the two-point integral

$$\begin{aligned} C_0^\pi \;&=\; \mathrm{Im}\int \frac{d^4p_\pi}{(2\pi)^4}\frac{1}{p_\pi^2 - m_\pi^2}\frac{1}{(P+K-p_\pi)^2 - M^2} \\ &=\; \frac{1}{8\pi}\frac{|\vec{p}_\pi|}{\sqrt{s}}, \end{aligned} \quad (45)$$

with $|\vec{p}_\pi| = \sqrt{\frac{(s-M^2+m_\pi^2)^2}{4s} - m_\pi^2}$; the three-point one

$$\begin{aligned} B_0^\pi \;&=\; \mathrm{Im}\int \frac{d^4p_\pi}{(2\pi)^4}\frac{1}{p_\pi^2 - m_\pi^2}\frac{1}{(k-p_\pi)^2 - m_\pi^2} \\ &\qquad \cdot\frac{1}{(P+K-p_\pi)^2 - M^2} \\ &=\; -\frac{1}{8\pi(s-M^2)}\ln\frac{2E_\pi}{m_\pi}, \end{aligned} \quad (46)$$

and finally, the four-point integral:

$$\begin{aligned} A_0^\pi \;&=\; \mathrm{Im}\int \frac{d^4p_\pi}{(2\pi)^4}\frac{1}{(k-p_\pi)^2 - m_\pi^2}\frac{1}{p_\pi^2 - m_\pi^2} \\ &\qquad \cdot\frac{1}{(k'-p_\pi)^2 - m_\pi^2}\frac{1}{(P+K-p_\pi)^2 - M^2} \\ &=\; \frac{1}{8\pi Q^2(s-M^2+m_\pi^2)} \\ &\quad \cdot\; \frac{1}{\sqrt{1+\frac{4m_\pi^2E^2}{Q^2p_\pi^2}}}\ln\frac{\sqrt{1+\frac{4m_\pi^2E^2}{Q^2p_\pi^2}}+1}{\sqrt{1+\frac{4m_\pi^2E^2}{Q^2p_\pi^2}}-1}. \end{aligned} \quad (47)$$

These integrals should however be reggeised as described in Section V by substituting the Regge propagator instead of the Feynman one. Denoting $t_1 = (k-p_\pi)^2$ and $t_2 = (k'-p_\pi)^2$ the momentum transferred by the pions in the t-channel, we have for the reggeized version of scalar integrals:

$$\begin{aligned} (C_0^\pi)^R \;&=\; \frac{1}{32\pi^2}\frac{p_\pi}{\sqrt{s}}\int d\Omega_\pi (t_1 - m_\pi^2)\mathcal{P}_\pi^R(\alpha_\pi(t_1)) \\ &\qquad \cdot(t_2 - m_\pi^2)\mathcal{P}_\pi^R(\alpha_\pi(t_2)) \end{aligned} \quad (48)$$

$$(B_0^\pi)^R = \frac{1}{32\pi^2}\frac{p_\pi}{\sqrt{s}}\int d\Omega_\pi (t_1 - m_\pi^2) \mathcal{P}_\pi^R(\alpha_\pi(t_1))\mathcal{P}_\pi^R(\alpha_\pi(t_2)), \quad (49)$$

$$(A_0^\pi)^R = \frac{1}{32\pi^2}\frac{p_\pi}{\sqrt{s}}\int d\Omega_\pi \mathcal{P}_\pi^R(\alpha_\pi(t_1))\mathcal{P}_\pi^R(\alpha_\pi(t_2)) \quad (50)$$

Similarly, in the case of the ρ-exchange in the s-channel, the integrals with non-zero imaginary part are:

$$C_0^\rho = \mathrm{Im}\int \frac{d^4p_\rho}{(2\pi)^4}\frac{1}{p_\rho^2 - m_\rho^2}\frac{1}{(P+K-p_\rho)^2 - M^2} = \frac{1}{8\pi}\frac{|\vec{p}_\rho|}{\sqrt{s}},$$

$$B_0^\rho = \mathrm{Im}\int \frac{d^4p_\rho}{(2\pi)^4}\frac{1}{p_\rho^2 - m_\rho^2}\frac{1}{(k-p_\rho)^2 - m_\pi^2}\cdot\frac{1}{(P+K-p_\rho)^2 - M^2} = -\frac{1}{8\pi(s-M^2)}\ln\frac{2E_\rho(s-M^2)}{Mm_\rho^2},$$

$$A_0^\rho = \mathrm{Im}\int \frac{d^4p_\rho}{(2\pi)^4}\frac{1}{(k-p_\rho)^2 - m_\pi^2}\frac{1}{p_\rho^2 - m_\rho^2}\cdot\frac{1}{(k'-p_\rho)^2 - m_\pi^2}\frac{1}{(P+K-p_\rho)^2 - M^2} = \frac{1}{8\pi Q^2(s - M^2 + m_\rho^2)}\frac{1}{\sqrt{1+\frac{4\sigma^2}{Q^2p_\rho^2}}}\cdot\ln\frac{\sqrt{1+\frac{4\sigma^2}{Q^2p_\rho^2}}+1}{\sqrt{1+\frac{4\sigma^2}{Q^2p_\rho^2}}-1}, \quad (51)$$

with $|\vec{p}_\rho| = \sqrt{\frac{(s-M^2+m_\rho^2)^2}{4s} - m_\rho^2}$, and $\sigma^2 = E^2m_\rho^2 - EE_\rho(m_\rho^2 - m_\pi^2) + \frac{1}{4}(m_\rho^2 - m_\pi^2)^2$. If neglecting the pion mass, $\sigma = \frac{Mm_\rho^2}{2s}$. The reggeization procedure is the same as for πN- intermediate state.

[1] M.K. Jones *et al.*, Phys. Rev. Lett. **84** (2000) 1398; O. Gayou *et al.*, Phys. Rev. Lett. **88** (2002) 092301.

[2] L. Andivahis *et al.*, Phys. Rev. **D 50** (1994) 5491; M.E. Christy *et al.*, Phys. Rev. **C 70** (2004) 015206; I.A. Qattan *et al.*, Phys. Rev. Lett. **94** (2005) 142301, [arXiv:nucl-ex/0410010].

[3] P.A.M. Guichon, M. Vanderhaeghen, Phys. Rev. Lett. **91** (2003) 142303.

[4] L.W. Mo and Y.S. Tsai, Rev. Mod. Phys. **41** (1969) 205; L.C. MAximon and J.A. Tjon, Phys. Rev. **C 62** (2000) 054320.

[5] P.G. Blunden, W. Melnitchouk and J.A. Tjon, Phys. Rev. Lett. **91** (2003) 142304.

[6] Y.C. Chen, A. Afanasev, S.J. Brodsky, C.E. Carlson and M. Vanderhaeghen, Phys. Rev. Lett. **93** (2004) 122301.

[7] N.F. Mott, Proc. R. Soc. London, Ser. **A135** (1935) 429; A.O. Barut and C. Fronsdal, Phys. Rev. **120** (1960) 1871; A. De Rujula, J.M. Kaplan and E. De Rafael, Nucl. Phys. **B 35** (1971) 365.

[8] S.P. Wells *et al.* [SAMPLE Collaboration], Phys. Rev. **C 63** (2001) 064001; F. Maas *et al.* [MAMI A4 Collaboration], Phys. Rev. Lett. **94** (2005) 082001.

[9] A. Afanasev, I. Akushevich and N.P. Merenkov, [arXiv:hep-ph/0208260].

[10] B. Pasquini and M. Vanderhaeghen, Phys. Rev. **C 70** (2004) 045206.

[11] L. Diaconescu and M. Ramsey-Musolf, Phys. Rev. **C 70** (2004) 054003.

[12] SLAC E158 Experiment, contact person K. Kumar; G. Cates, K. Kumar and D. Lhuillier, spokespersons HAPPEX-2 Experiment, JLab E-99-115; D. Beck, spokesperson JLab/G0 Experiment, JLabE-00—6, E-01-116.

[13] M. Gorchtein, P.A.M. Guichon and M. Vanderhaeghen, Nucl Phys. **A 741** (2004) 234.

[14] A.V. Afanasev, N.P. Merenkov, Phys. Lett. **B 599** (2004) 48; Phys. Rev. **D 70** (2004) 073002.

[15] D. Drechsel, B. Pasquini, and M. Vanderhaeghen, Phys. Repts. 378 (2003) 99.

[16] R.E. Prange, Phys. Rev. **110** (1958) 240.

[17] R.A. Berg and C.N. Lindner, Nucl. Phys. **26** (1961) 259.

[18] A.I. L'vov, V.A. Petrun'kin, M. Schumacher, Phys. Rev. **C 55** (1997) 359.

[19] D. Drechsel, M. Gorchtein, B. Pasquini, M. Vanderhaeghen, Phys. Rev. **C 61** (1999) 015204.

[20] B. Pasquini, M. Gorchtein, D. Drechsel, A. Metz, M. Vanderhaeghen, Eur. Phys. **A 11** (2001) 185.

[21] M. Gorchtein, PhD thesis, Universität Mainz.

[22] T.H. Bauer, R.D. Spital, D.R. Yennie and F.M. Pipkin, Rev. Mod. Phys. **50** (1978) 261; [Erratum-ibid. **51** (1979) 407].

[23] M. Guidal, J.-M. Laget, M. Vanderhaeghen, Nucl. Phys. **A 627** (1997) 645.

[24] A. Metz and D. Drechsel, Z. Phys. **A 356** (1996) 351; A. Metz, PhD Thesis, Universität Mainz.

[25] G. Passarino and M. Veltman, Nucl. Phys. **B160** (1979) 151.